Suggestion from Analysis of TRMM

Yukari N. Takayabu
National Institute for Environmental Studies, Tsukuba, Japan

1. Introduction

The understanding of the behaviour of the cloud and precipitation systems and their interaction with the large-scale climate is indispensable in understanding the climate system. Recent new technologies for satellite observations have been provided us with various data which largely help us understand the dynamics of cloud and precipitation systems and also their large-scale effects.

Here we first introduce the paper *"the Abrupt Termination of the 1997-1998 El Niño in Response to a Madden-Julian Oscillation"*, (Takayabu et al. 1999), as an example of the interaction between the large-scale tropical precipitation system and the El Niño dynamics. Then, using the data from space-borne preciptation radar (PR) implemented on the Tropical Rainfall Measuring Mission (TRMM) satellite, we show the precipitation property of this large-scale precipitation system and its dynamical implications.

A Madden-Julian oscillation (MJO; Madden and Julian, 1971, 1972) is a global-scale (20,000-40,000km) atmospheric disturbance that propagates eastward in the equatorial region with an intraseasonal (35-90days) time scale, and usually coupled with a large-scale convective activity over the warm water pool region from the Indian Ocean to the Western Pacific (Wang and Rui, 1990). Previous studies suggest the importance of MJO in the El Niño and Southern Oscillation (ENSO) dynamics, concerning the roles of MJOs in accelerating the El Niño developments through the westerly wind bursts (*e.g.* Lau and Chan 1986; Nitta and Motoki 1987; Kindle and Phoebus 1995). However, MJOs have not been succesfully simulated in the atmospheric general circulation models yet, which means that we still do not understand the dynamics of MJO properly.

The 1997-98 El Niño was one of the largest events in this century. The life cycle of this event was succesfully monitored with the TOGA-TAO array of moored buoys (McPhaden, 1999). On the initiation of the event, he emphasized the triggering roles of repetitive occurences of the westerly wind bursts over the western Pacific warm pool region associated with the MJO. In relation with the termination of the event, he indicated that the sea surface temperature (SST) over the eastern equatorial Pacific suddenly dropped in May 1998 accompanying the abrupt intensification of the easterly trade winds. However, what caused such intensification of the trade winds was not known.

By analyzing the satellite-observed global precipitation data, SST data, and the atmospheric global analysis data, we found that an exceptionally robust precipitation system associated with the MJO propagated the complete equatorial circle in May 1998. It is indicated that the propagation of this MJO caused the intensification of the easterly trade winds that induced the equatorial ocean upwelling and accelerated the termination of 1997-98 El Niño .

Statistics with the vertical rain profile data of TRMM PR2A25 revealed that the stratiform rain was dominant in the large-scale precipitation system of this MJO. This results implies the shallowness of the diabatic heating which may explain the equivalent depth of 20m that was obtained from the organization features of cloud systems.

2. Data

Following data are utilized in this study:

(1)Global precipitation data over the ocean were produced by Frank Wentz of Remote Sensing Systems from Special Sensor Microwave/Imager (SSM/I) (Wentz, 1998) at 0.25×0.25 longitude-latitude grids. We used precipitation data from three DMSP satellites avialable for our analysis period to construct daily averages.

(2)Daily sea surface temperature (SST) data utilized in this study were retrieved from

Corresponding author address: Yukari N. Takayabu, National Institute for Environmental Studies, 16-2 Onogawa, Tsukuba, Ibaraki 305-0053, JAPAN email: yukari@nies.go.jp

TMI (TRMM Microwave Imager) data at 0.25×0.25 longitude-latitude grids with an algorithm developed by Shibata (1999); and three-day running means were taken to smooth out the noise.

(3)Wind data were obtained from the global analysis data set produced by the European Centre for Medium-Range Weather Forecast (ECMWF). Twice daily data at 2.5×2.5 longitude-latitude grids were utilized.

(4)Precipitation data were also obtained from TRMM PR. It has an advantage of measuring the vertical rain profiles, either over the ocean or over the land. Utilizing the vertical radar profiles, the discrimination of the stratiform rain from the convective rain is performed in the 2A23 algorithm (Awaka et al. 1998). We utilized PR2A25 data with this rain property flag for the rain statistics with the May 1998 MJO event.

3. Results

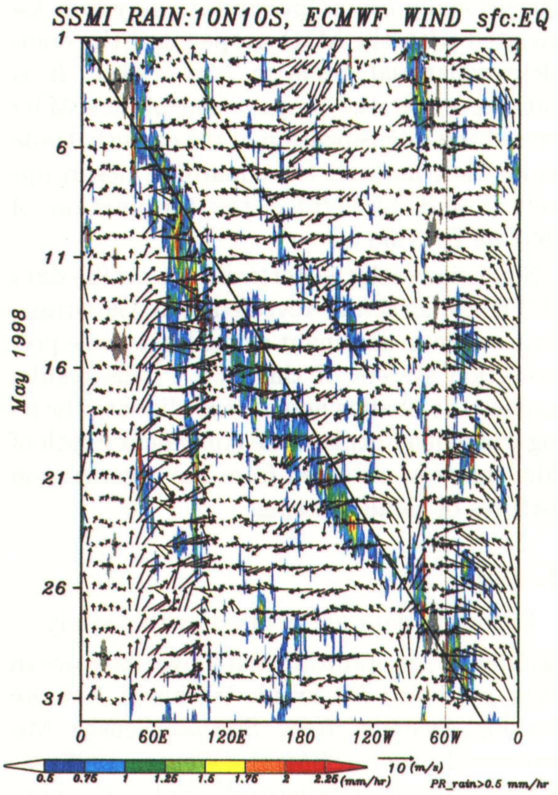

Fig. 1 Time versus longitude sections of the rain rate averaged from 10°N to 10°S and the ECMWF surface wind vectors on the equator for the period of May 1 - June 1, 1998. For the rain rate data, SSM/I precipitation were primarily used. The undefined values over land (around 10°-40°E and around 80°-50°W) were interpolated with the TRMM PR data. (Takayabu et al. 1999, *Nature)*

Figure 1 shows a longitude-time section of SSM/I rain rate averaged for 10°N-10°S. The rain data over land are interpolated with the PR precipitations. A remarkable eastward propagation of a global wavenumber-one precipitation system is observed completing the global equatorial circle in about 33 days starting from near the Greenwich meridian at 1 May (solid line). About one week prior to this system, a propagation of a weaker rain system with a similar speed was observed (dashed line).

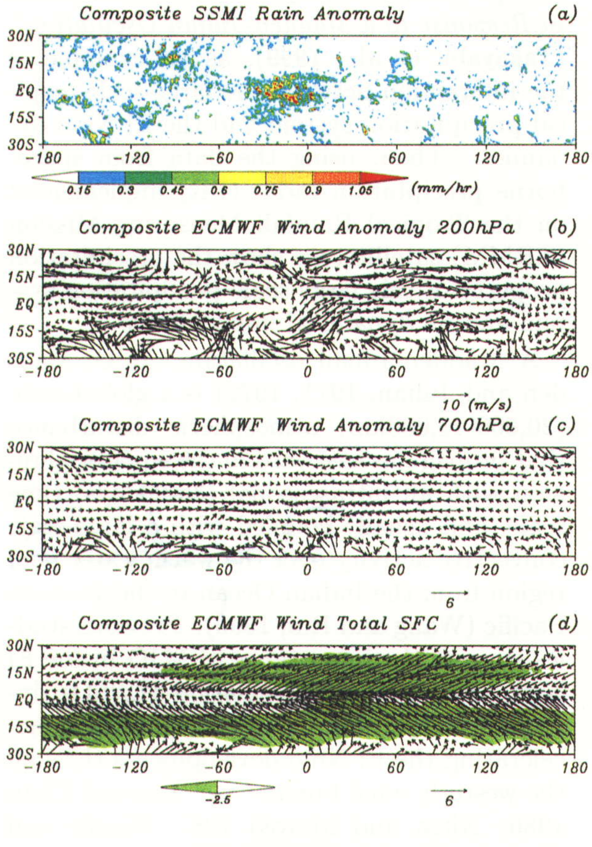

Fig. 2 Composited SSM/I precipitation (a) ECMWF horizontal winds at 200 hPa (b), at 700 hPa (c), and at the surface (d). For the precipitaion, and the 200 hPa and 700 hPa winds, anomalies from the zonal means are depicted. For the surface, the total winds are depicted with vectors and the zonal winds less than -2.5m s^{-1} are shaded. The solid line in Fig. 1 shows the composite base longitudes. The abscissa is the relative distance in longitude from the composite center and the ordinate is the real latitudes. (Takayabu

et al. 1999, *Nature)*

Leading these propagating precipitation systems, intensifications of the easterly winds are noticed especially in the region from 120°E to 100°W over the Pacific Ocean. The intensified trade winds accompanying the first weaker rain system initiated the cold water to appear on the surface in the region of 110°-130°E at around 13 May. Then, the second intensification of the trade winds accompanying the following major system, indicated with a solid line, caused the westward expansion of the cold tongue in 18-20 May.

A composite structure of this significant system is shown in Fig. 2. Base longitudes for composites follow the propagation of the major precipitation system indicated by the solid line in Fig. 1. Figure 2(a) shows the composite for SSM/I precipitation. The primary feature is the zonal wavenumber-one structure. The zonal extension of the major rain system is about 60 degrees in longitude. The precedent rain system that initiated the cold tongue is also noticed about 60 degrees to the east of the composite center.

Anomalous winds at 200 hPa (Fig. 2(b)) cleary exhibit a so-called 'Matsuno-Gill pattern' (Matsuno 1966, Gill 1980): with the equatorial Rossby wave response to the west and the Kelvin wave response to the east of the precipitation center. In the lower troposphere, at 700 hPa, on the other hand, the Rossby wave response diminishes and the Kelvin wave sturucture becomes dominant. The frictional Ekman convergence at the surface accompanies the lower-tropospheric Kelvin wave disturbance superposed on the mean easterly winds. The corresponding surface winds show a comspicuous intensification of the easterly components in the eastern hemisphere relative to the precipitation center. The wavenumber-one component is dominant also in this field. We can confirm the intensified easterly winds at the equator, which are considered to force the equatorial ocean upwelling, at around +25° and +90° relative longitudes as indicated with shades. Another significant feature is the strong wind convergence toward the equator in the relative eastern hemisphere. This is the Ekman convergence associated with the easterly winds. The convergence centers are along 5°N and 5°S. It is considered that water-vapor-rich belts are produced ahead of the precipitation area and maintained the eastward propagation of the system.

Here are two issues raised concerning this MJO event. One is why this MJO had a Kelvin wave structure in the lower troposphere instead of the 'Matsuno-Gill pattern', which was essential for this MJO to put an impact on the termination of the El Niño. The other is what determined the propagation speed of this MJO.

For the former question, we can find an explanation that the mean zonal-wind shear playing a role in determining its dynamical structure. Wang and Xie (1996) theoretically studied the effects of the mean wind shear on the atmospheric equatorial waves. They indicated that the westerly wind shear (stronger westerly wind upward) traps the Rossby waves in the upper troposphere, while not much affects the Kelvin waves. In our case, the mean zonal-wind difference between 200 hPa and 850 hPa was 6.7 $\mathrm{m\,s^{-1}}$, which is comparable to 5 $\mathrm{m\,s^{-1}}$ they assumed.

Thus, the mean wind field not only allowed the global propagation of a convectively-coupled MJO, but also affected its structure suppressing the Rossby wave response in the lower troposphere. The resultant lower-tropospheric Kelvin wave disturbance superposed on the mean easterly winds, in turn, caused the intensification of the easterly trade winds, and brought about an unusual easterly-wind-impact of MJO on El Niño.

As for the propagation speed, the previous studies indicate the oscillation period of MJOs as 35-90 days. It is usually considered that their propagation consists of the slower-speed system which is coupled with convection over the warm water pool region and the faster-speed dry wave over the western hemisphere. Then, it is puzzling that the MJO in May 1998 had the fastest speed among the MJOs, 33 days to complete the equatorial circle, even if this case was always coupled with convection.

Considering the lower-level structure of this system appeared to be a Kelvin-wave structure, this speed of ~14m/s is consistent with the previous spectral statistics which indicated the equivalent depth of ~20m of the equatorial waves appearing in the cloud field (Takayabu 1994, Wheeler and Kiladis 1999).

However, this shallow equivalent depth itself has not been explained quantitatively enough.

Concerning the tropical disturbance coupled with convection, the vertical profile of the latent heating is very important to understand the effects of convection. For the tropical convective system, Houze (1982) indicated that there are two typical diabatic heating profiles attributed to the latent heating; one is related to the convective rain and the other is related to the stratiform (anvil) rain. The former has the heating maximum in the mid-troposphere while the latter has the heating in the upper troposphere and the cooling in the lower troposphere. Consequently, the convective rain induces the dynamical disturbance which has the out-of-phase relationship in the wind and the pressure field, while the anvil rain induces the higher-order vertical profile. Therefore, discrimination between the convective rain and the stratiform rain is essential in understanding the interaction between the dynamical disturbances and the precipitating systems.

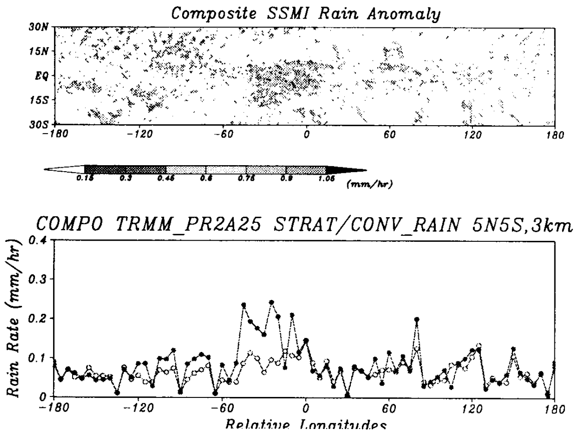

Fig. 3 Composited SSM/I precipitation (upper), and PR2a25 rain rates at 3km (lower). The method of composite is the same as that for Fig. 2. In the lower panel, the stratiform rain rates are marked with closed circles and the convective rain rates are marked with open circles.

TRMM PR data do not directly observe the latent heating profiles, but do provide us with the rainrate profiles. Here, we made a composite of convective rain and the stratiform rain separately to discuss its implication to the dynamical features of the MJO. Figure 3 is the same composite of the MJO as Fig. 2 but with the convective rain and the stratiform rain at 3km, averaged from 5°N to 5°S. The upper panel is same as the Fig. 2(a) just for comparison convenience. The total ratio in this latitude belt between the stratiform rain and the convective rain is 56:44. In the leading edge of the rain system of this MJO (-5°- +10°relative longitude) the stratiform/convective ratio is 49:51, while in the trainling region in -50°- -5°RLON the stratiform rain dominates by 66:34. Outside of this primary rain area, the ratio was close to 50:50.

Figures 4 show the vertical profiles of the composite total, stratiform, and convective rain in the four regions relative to the MJO. In the primary rain area (Figs. 4(b) and 4(c)), the rain rate is about twice as large as the outside. In the leading edge, the stratiform and the convective rain have almost the same strength. In the trailing region, the convective rain reduces its strength and the stratiform (anvil) rain dominates.

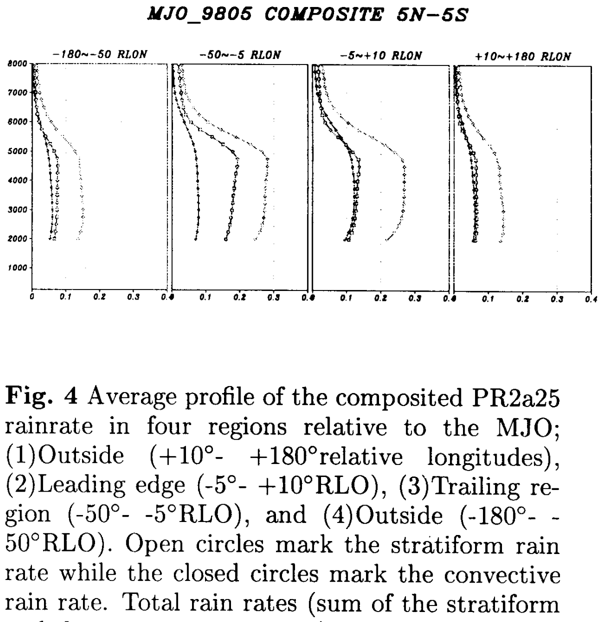

Fig. 4 Average profile of the composited PR2a25 rainrate in four regions relative to the MJO; (1)Outside (+10°- +180°relative longitudes), (2)Leading edge (-5°- +10°RLO), (3)Trailing region (-50°- -5°RLO), and (4)Outside (-180°- -50°RLO). Open circles mark the stratiform rain rate while the closed circles mark the convective rain rate. Total rain rates (sum of the stratiform and the convective rain rate) are also depicted.

4. Discussions

What does the dominance of the stratiform rain in this MJO system imply? We showed that the MJO in May 1998 had a structure of Kelvin wave in the lower troposphere and propagated with a speed of ~14m/s. It corresponds to the Kelvin wave with the equivalent depth of ~20m , which is consistent with the results of previous spectral analyses with the satellite infrared observations. This means that the vertical wavelength of the atmospheric disturbance is ~9km, which has been considered too small if we assume the convective rain heating profile to be dominant. However, when the stratiform rain is dominant, we can expect the heating profile with warming in the upper troposphere and cooling in the lower troposphere. If this tropospheric second baroclinic vertical mode is controlling the phenomena, we can explain the shallowness of the equivalent depth.

Indeed, we need further studies to quantify the latent heating and also radiative heating profiles associated with large-scale precipitating systems as shown here.

5. Summary and Conclusions

The results are summarized as follows:

1. An MJO in May 1998 traveled around the complete equatorial circle in 33 days, always accompanied by a large-scale precipitation system. It had a Kelvin-wave structure in the lower troposphere and accelerated the termination of the 1997-98 El Niño through the easterly-wind intensification. The propagation speed was ~14m/s, which agrees with that of the 'convective Kelvin wave' with the equivalent depth of ~20m suggested by Takayabu (1994) and Wheeler and Kiladis (1999).
2. Precipitation properties associated with this MJO were studied utilizing TRMM PR2A25 data. Stratiform rain dominated the convective rain in the large-scale (~7000km) rain system of this MJO by 63:37. This result partly explains the shallow equivalent depth (h~20m) of the tropical convective system suggested in the previous studies.

It is concluded that first, the importance of understanding multi-scale interaction in the climate system was reemphasized. Secondly, it is essential to know the vertical structure of the diabatic heating (radiative heating as well as the latent heating) to understand the dynamics of the large-scale convective systems. For that purpose, space-borne vertical profilings of the cloud microphysics would provide us with valuable data.

Acknowledgements

The author is grateful to Drs. Toshio Iguchi, Misako Kachi, Akira Shibata, Tetsuo Nakazawa, and Hiroshi Kanzawa for the availability of TRMM and SSM/I data, as well as for fruitful discussions. She is also indebted to Dr. Yasushi Suzuki and Mr. Hatsuki Fujinami for helping her with processing the TRMM data.

References

Awaka, J., T. Iguchi, and K. Okamoto, 1998: Early results on rain type classification by the Tropical Rainfall Measuring Mission (TRMM) precipitation radar, *Proc. 8th URSI Commission F Open Symp., Aveiro, Portugal*, 143-146.

Gill, A.E., 1980: Some simple solutions for heat-induced tropical circulation, *Q. J. R. Meteorol. Soc.*, **106**, 447-462.

Houze, R. A., Jr., 1982: Cloud clusters and large-scale vertical motions in the tropics, *J. Meteor. Soc. Japan*, **60**, 396-410.

Kindle, J. C. and Phoebus, P. A., 1995: The ocean response to operational westerly wind bursts., *J. Geophys. Res.*, **100**, 4893-4920.

Lau, K.-M., and P. H. Chan, 1986: Aspects of the 40-50 day oscillation in the northern winter as inferred from outgoing longwave radiation. *Mon. Wea. Rev.*, **114**, 1354-1367.

Madden, R.A. and Julian, P.R., 1971: Detection of a 40-50 day oscillation in the zonal wind in the tropical Pacific. *J. Atmos. Sci.*, **28**, 702-708.

Madden, R.A. and Julian, P.R., 1972: Description of global scale circulation cells in the tropics with a 40-50 day period, *J. Atmos. Sci.*, **29**, 1109-1120.

Matsuno, T., 1966: Quasi-geostrophic motions in the equatorial area. *J. Meteorol. Soc. Japan*, **44**, 25-43.

McPhaden, M. J., 1999: Genesis and evolution of the 1997-98 El Nino. *Science*, **283**, 950-954.

Nitta, Ts. and Motoki, T., 1987: Abrupt enhancement of convective activity and low level westerly wind burst during the onset phase of 1986-87 El Nino. *J. Meteorol. Soc. Japan*,**65**, 497-506.

Shibata, A., Imaoka, K., Kachi, M., and Murakami, H., 1999: SST observation by TRMM Microwave Imager aboard Tropical Rainfall Measuring Mission. *Umi no Kenkyu*, **8**, 135-139. (In Japanese)

Takayabu, Y. N., T. Iguchi, M. Kachi, A. Shibata, and H. Kanzawa, 1999: Abrupt termination of the 1997-98 El Niño in response to a Madden-Julian oscillation, *Nature*, **402**, 279-282.

Wang, B. and Rui, H., 1990: Synoptic climatology of transient tropical intraseasonal convection anomalies. *Meteorol. Atmos. Phys.*, **44**, 43-61.

Wang, B. and Xie, X., 1996: Low-frequency equatorial waves in vertically sheared zonal flow. Part I: Stable waves, *J. Atmos. Sci.*, **53**, 449-467.

Wentz F. J., and Spencer, R. W., 1998: SSM/I rain retrievals within a unified all-weather ocean algorithm, *J. Atmos. Sci.*, **55**, 1613-1627.